Manuscript refereed by Prof Ilaria Cristofolini (Trento University, Italy)

Processing and Corrosion Behaviour Of Metal Powder Blends In LPBF

Michael Norda[1] michael.norda@ifam.fraunhofer.de, Marie Luise Köhler[2] m.koehler@iwm.rwth-aachen.de, Simone Herzog[2], Christoph Broeckmann[2], Frank Petzoldt[1]

[1]Fraunhofer Institute for Manufacturing Technology and Advanced Materials IFAM, Wiener Straße 12, 28359 Bremen, Germany
[2]RWTH Aachen University, Institute for Materials Applications in Mechanical Engineering (IWM), Augustinerbach 4, 52062 Aachen, Germany

Abstract

Laser Powder Bed Fusion (LPBF) has become an attractive alternative to conventional processing routes over the past years. While some alloys are already processed in series production, the overall amount of available materials is low. Due to the high price of specially atomized powders, material variation is often neglected. This work covers the blending, in-situ processing and testing of metal powder blends and the produced specimen. Different metal powders are blended to create a Super Duplex Steel. The powder blend quality is assessed by different methods. Heat treatments, corrosion tests and EDX analyses determine the specimen quality as well as tensile tests. The properties of the created alloy are compared to conventionally manufactured duplex and super duplex steels in order to show the potentials of this approach.

Introduction

There has always been a lack of availability in materials for special applications in powder bed additive manufacturing (AM). Producing metal powder in small batches is intense in costs and time. Thus, users have to choose between non-tailored materials and high prices. One kind of those materials for special applications are Duplex steels, which combine high strength with high toughness due to the typical austenite-ferrite mixed structure. Super-duplex steels have increased contents of chromium, molybdenum and nitrogen to achieve seawater resistance (1). This work investigates the corrosion behaviour of specimens, which were fabricated by Laser Powder Bed Fusion (LPBF) and tailored super duplex steel powder blends. The goal of these powder blend approach is a tailored configuration of specific component properties by adding certain element powders to a specific base AM powder.
It is possible to process and change the properties of steel alloys by using commercially easily available element powders and master alloys. Due to the high energy input of the laser printing process into the material, which heats it up to above the liquidus temperature, it is possible to produce alloys within the process by melting (2). Through variations of element powders (powder construction kit), the component developer is no longer dependent on the narrow portfolio of powder suppliers, but can select individually and produce his own alloys and material properties.
Laser beam-based processing of elemental powders enables design freedom in combination with material diversity. The approach of processing element powders by means of laser cladding (LMD) is widespread, since no segregation problems can occur in the powder bed. However, the geometric flexibility and accuracy of this process is limited compared to LPBF. Examples of important research work are the production of the stainless steels X2CrNiMo17-12-2 and X14CrMoS17 (430L) (3), element powder LMD for rapid material developments (4) or developments for graded steels (5). Prior publications about this research project have shown that the segregation of powder blends in powder bed additive manufacturing processes is low, when using certain parameters and methods (6).

Materials and methods

Powders & parts

Two duplex alloy compositions (D1 & D2) similar to a standard corrosion resistant super duplex steel (1.4501) were chosen and realized by blending four and five commercially available powders, respectively. The alloys are based on 1.4462 and modified by additions of 1.4404, Cr, CrN and Mo. All powders have a spherical shape whereas the CrN powder is mechanically crushed with an irregular shape. The mixing ratios of the two alloys can be found in Table 1.

Table 1: Mixing ratio of blends in weight %

Name	1.4462 (D2205)	1.4404 (316L)	CrN	Mo	Cr
60:30:2:2:6 (D1)	60,00	30.00	2.00	2.00	6.00
75:18:2:5 (D2)	75.00	18.00	2.00	-	5.00

The mixing duration and methodology was selected based on prior works (6). According to these, the Turbula mixer (three-dimensional shaking mixing) provides sufficient mixing of the powder after a mixing time of 15 minutes. The blends “60:30:2:2:6” and “75:18:2:5” were blended for 30 minutes. The alloying content of the powders and the calculated composition from the mixing ratio is listed in Table 2. The nominal composition of the 1.4501 is provided for comparison.

Table 2: Calculated chemical composition of utilized base steels and the powder mixtures in weight %

Name	C	Cr	Mo	Ni	N	Si	Mn
1.4462 (D2205)	≤ 0.03	22,00	3,00	5.25	0.16	≤ 1.00	≤ 2.00
1.4404 (316L)	≤ 0.03	17.50	2.50	12.50	-	1.00	2.00
CrN	-	78.8	-	-	21.2	-	-
Cr	-	100	-	-	-	-	-
Mo	-	-	100	-	-	-	-
60:30:2:2:6 (D1)	0.02	26.03	4.48	6.75	0.54	0.45	0.9
75:18:2:5 (D2)	0.02	26.20	2.66	6.20	0.55	0.47	0.9
1.4501	≤ 0.03	25	3,5	7	0,25	≤ 1	≤1

Table 3: PSD of the utilized powders and blend

Name	D10 [µm]	D50 [µm]	D90 [µm]
1.4462 (D2205)	28.3	43.5	62.1
1.4404 (316L)	20.7	35.8	54.3
CrN	21,8	59,7	99,0
Cr	21.0	37.2	54.0
Mo	5.6	15.5	38.3
60:30:2:2:6 (D1)	23.6	41.9	61.7
75:18:2:5 (D2)	25.0	40.9	59.3

According to Shenoy the influence of particle size is considered to be the most important concerning segregation (7). The publication prior to this work confirmed the conclusions (6). The particle size distribution of the powders used for the blends in this work were determined by a Particle size measuring device from Beckman Coulter LS. The particle size distributions of the utilized powders is provided in Table 3. The mechanically crushed CrN powder is slightly coarser than the 1.4462 and 1.4404, while the Mo powder is finer. The SEM and EDX images identify the different elements on a qualitative basis. Figure 1 shows that the blended elements can be found well distributed all over the screened scene of D1. Furthermore, it confirms that the Mo powder is much finer than the others. Figure 2 helps to identify the elements of D2. There is no Mo element powder, therefore the Ni analysis is illustrated, which helps to distinguish the 1.4462 from the 1.4404. The brighter green particles contain higher Ni, which identifies them as 1.4404.

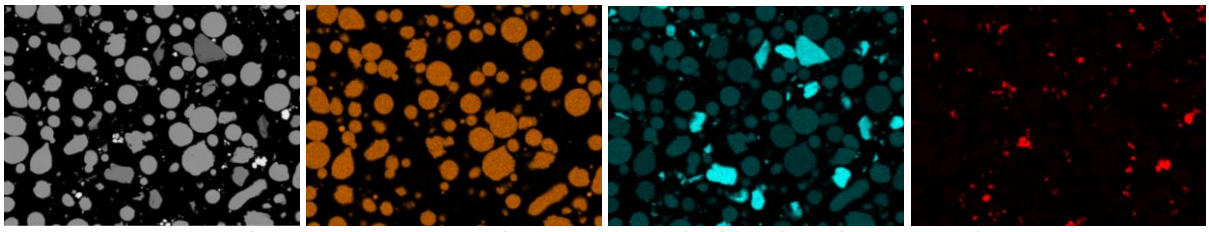

Figure 1. REM + EDX images of powder blend D1 (60:30:2:2:6)

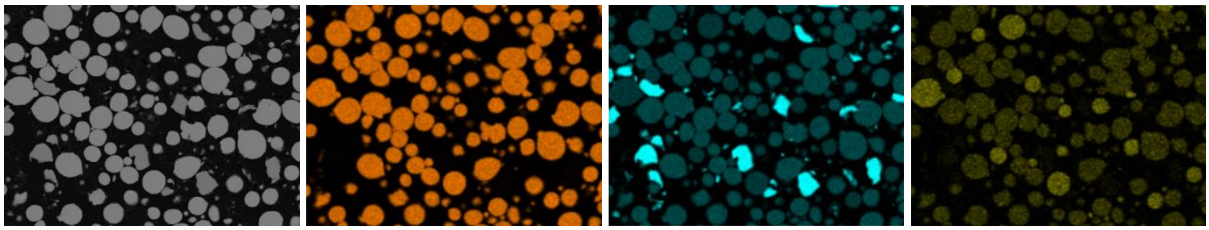

Figure 2. SEM + EDX images of powder blend D2 (75:18:2:5)

The materials (1.4462; D1; D2) were processed on a Trumpf TruPrint 1000 with a beam focus of 30 µm. The parameters were fixed for all samples: a laser power of 195 W, a scan speed of 800 mm s^{-1} and a hatch distance of 50 µm. In combination with a layer thickness of 40 µm an energy density of 122 J mm^{-3} results for manufacturing these parts. Two build jobs were manufactured, one for the tensile specimen in X and Z direction and one for cubes (10x10x10 mm) and a plate (50x10x1 mm) for the corrosion tests. In the following, half of the specimens of each blend received a diffusion annealing (DA) at 1270 °C for 2 h. Afterwards, each specimen including the ones from diffusion annealing were solution annealed (SA) in respect to their specific alloy composition. The temperatures were calculated by Thermocalc (8), which recommended 1060 °C for steel 1.4462, 1070 °C for D1 and 1120 °C for D2.

Blend and Part Analysis

A quantitative wet chemical analysis was conducted for blend D1 in order to find the actual chemical composition of the blend and verify the calculated values. In order to examine the composition of the parts an EDX analysis was carried out. Since super duplex steels are meant for environments causing corrosion, they are naturally very resistant against it. Therefore, the blends were analysed using a current density potential curve. The tests were conducted using a 3.5 % NaCl solution at room temperature. Each specimen´s surface was ground and polished. As reference, parts made of the base powder 1.4462 and externally purchased, conventionally manufactured parts of 1.4662 and 1.4501 were compared to the blends. The tensile tests were conducted at room temperature using B4x20 specimen according to DIN 50125. Only samples of D1 and D2 in solution annealed condition were tested and compared to the values of 1.4501 from literature. Furthermore, the three specimens were built in laid (X) and standing (Z) direction, respectively. An overview can be found in Table 4.

Table 4: Speicmen Analysis Overview

Analysis	Diffusion annealed	Solution annealed	Curr. density/ pot. curve	Tensile Tests
D1 part (LPBF + SA)	-	X	X	X
D1 part (LPBF + DA + SA)	X	X	X	-
D2 part (LPBF+ SA)	-	X	X	X
D2 part (LPBF + DA + SA)	X	X	X	-
1.4462 (LPBF + SA)	-	X	X	-
1.4462 (LPBF + DA + SA)	X	X	X	-
1.4462 (conventional)	-	-	X	-
1.4501 (conventional)	-	-	X	-

Results

Wet chemical analysis

The resulting values from the wet chemical analysis are listed in Table 5. It shows that the actual values are slightly higher in Cr, Mo, Mn and Si. The content of Ni is moderately lower. N is 50 % lower as it has been calculated, which can be related to the solubility of nitrogen in iron (9). The higher content of Cr can be connected to slightly wrong amount of ingredients used for the blend.

Table 5: Results of wet chemical analysis in weight %

Name	C	Cr	Mo	Ni	N	Si	Mn
D1 – calculated	0.02	26.03	4.48	6.75	0.54	0.45	0.90
D1 – analysed	0.02	27.02	4.82	6.23	0,24	0.59	1,14

Composition of LPBF parts

The results of one EDX measurements are provided in Table 6 and Table 7. The measured and calculated powder compositions are provided as reference, respectively. Several different positions where analyzed (Figure 3 and Figure 4). It can be seen that all values are very similar to the powder values from the wet chemical analysis. Cr is again slightly increased, while the other elements are very close to their individual target values. As said before, this can be related to the slightly wrong amount of ingredients used for the blend. The findings lead to the conclusion that the different powders, including the elemental one, are well melted and mostly homogeneously distributed within the volume of the sample. This also confirms the findings of the wet chemical analysis of the blend D1. Figure 3 and Figure 4 show an area of roughly 120 x 120 µm², which equals four scan vectors of the laser. A few non-melted particles were found. Those appear very locally and are probably related to their original size. Smaller particles need less energy to dissolve into the matrix of the specimen. The laser spot has a diameter of 30 µm and exposure time is very short (800 mm/s) and the heat transfer can cover only a certain area in this period (10). If there are only a few particles of this kind, no major impact on the material properties is expected. Nevertheless, parameters should be designed to reduce this phenomena.

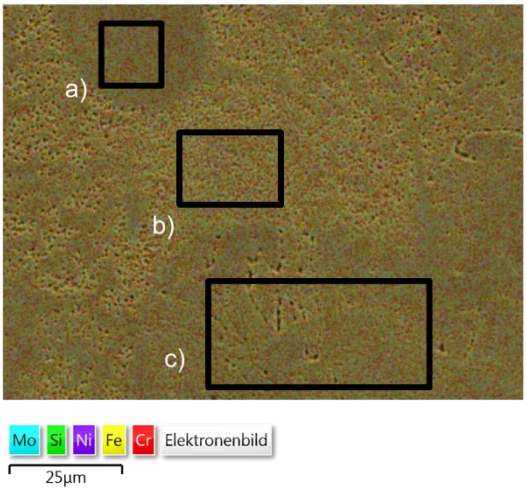

Figure 3. D1 - EDX measured areas

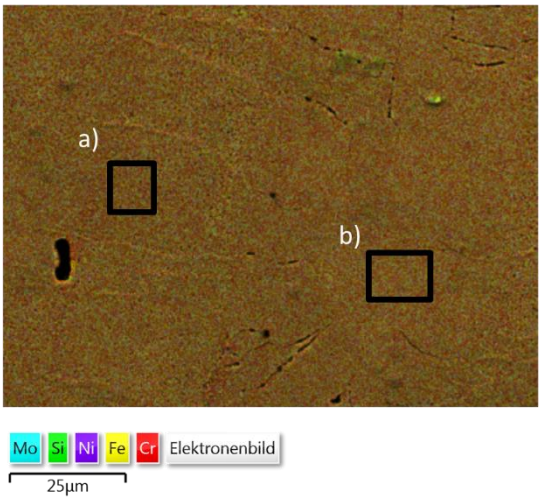

Figure 4. D2 - EDX measured areas

Table 6: D1 - Measured chemical compositions by EDX

Element	a) %	b) %	c) %	powder % (analysed)
Si	0.64	0.62	0.63	0.59
Cr	27.67	27.74	26.80	27.02
Fe	Bal	Bal	Bal	Bal
Ni	6.55	6.62	6.83	6.23
Mo	4.44	4.73	4.68	4.82

Table 7: D2 - Measured chemical compositions by EDX

Element	a) %	b) %	powder % (calculated)
Si	0.66	0.67	0.47
Cr	28.64	28.18	26.20
Fe	Bal	Bal	Bal
Ni	5.71	6.09	6.20
Mo	2.65	2.49	2.66

Corrosion results

As reference, Figure 5 shows the corrosion behaviour of both conventionally manufactured 1.4462 and 1.4501. Although 1.4501 has higher content of Cr, Mo and Ni, the current density increases at a lower potential, the passivation starts slightly earlier than 1.4462 but with higher potential the values cover themselves. The 1.4501 reaches its critical pitting corrosion potential slightly earlier than 1.4462. Compared to that, Figure 6 illustrates the values of the conventionally manufactured to the LPBF manufactured 1.4462 alloy. The results show that the LPBF parts are much more sensitive for corrosion since the current density is higher at each point of the analysis. The diffusion annealing can shift the corrosion to a slightly higher potential but still the corrosion resistance is much lower than conventional parts. The results show that the LPBF process itself has a big impact on corrosion

behaviour already. In other works, the influence of the LPBF process of the corrosion behaviour of AISI 316L was investigated. It has shown similar resistance to corrosion in cast (11), rolled and LPBF condition (12). The parameters, which were identified as most influential, were porosity and defects. Since the density was measured with 98.5%, it is likely that the LPBF parameters used in this work lead to higher porosity and defects compared to conventionally manufactured parts. This would explain the decreased corrosion resistance of the LPBF parts in prealloyed (1.4462) and blended condition (D1&D2).

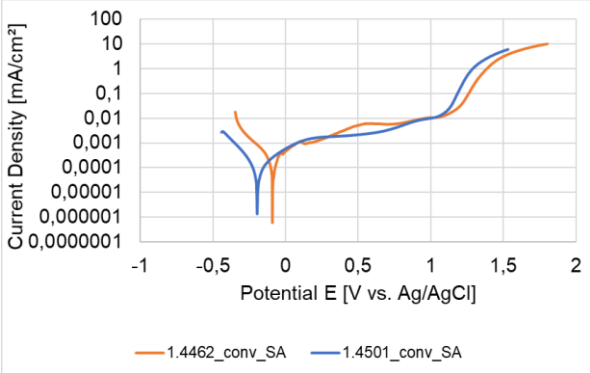

Figure 5. Corrosion behaviour conventional steels

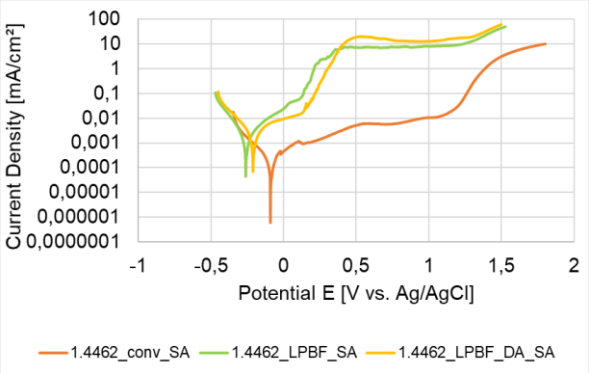

Figure 6. Corrosion behaviour conventional vs. LPBF

Since Figure 6 shows that the LPBF process has such an intense influence on the material properties, the blends D1 and D2 are compared to the prealloyed and LPBF-manufactured 1.4462, only. Figure 7 compares D1 and 1.4462. The values indicate that the diffusion annealing strengthens the corrosion resistance compared to the as built specimens. Also, the corrosion resistance increased relative to 1.4462 alloy. This signals that the corrosion resistant elements are more homogenously distributed within the matrix of the specimen after the heat treatment (13). Without diffusion annealing after the build process, the specimens show higher current densities between 0 and 0.25 V than any other parts. The critical pitting corrosion potential is reached first by the as built and solution annealed specimen. The others show the critical potential at around 1.25 V.
Figure 8 shows the corrosion behaviour of D2 compared to the LPBF 1.4462. Here the corrosion behaviour is very similar and the added elements only have a small positive impact on corrosion resistance.

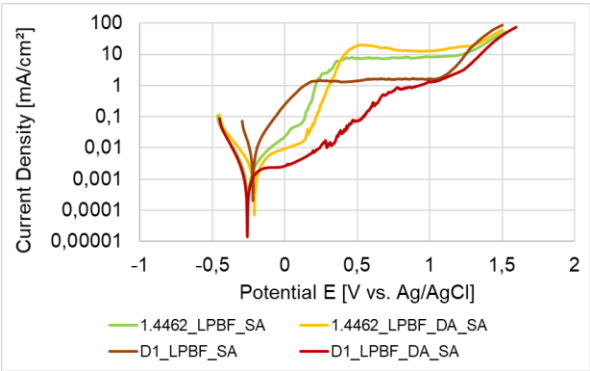

Figure 7. Corrosion behaviour prealloyed powder vs. blend D1

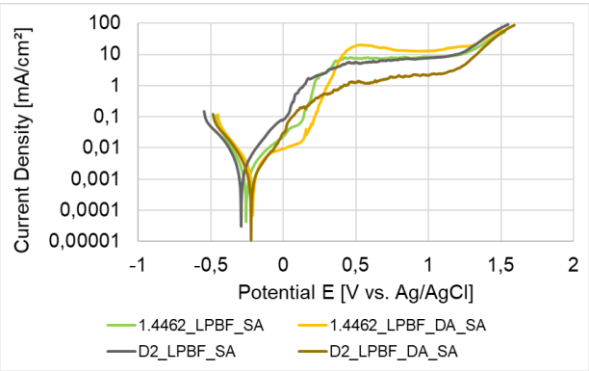

Figure 8. Corrosion behaviour prealloyed powder vs. blend D2

Tensile Tests

Figure 9 illustrate the stress-strain curves while Table 8 shows the average results (x) including standard deviation (s) of the D1 blend in X and Z direction compared to the targeted values from conventionally manufactured1.4501. The tensile strength Rm and Rp 0.2 values of D1 are within the tolerances of 1.4501. Only the elongation is lower than expected from this material. Early failure in this case can be due to the flaws in the material but also due to the presence of intermetallic phases rich in Cr and Mo (14). The Young´s modulus was found by the stress-strain curve and can be inaccurate. The Young´s Modulus of the Z-specimen does not reach 200 kN/mm in average, and the standard deviation twice as high as of the X-specimen. Since all values of the Z-specimen are lower this is probably caused by the anisotropic material behaviour of LPBF parts. That behaviour is generally

caused by the rapid melting and solidification process (15). Generally, load in direction of the layers needs to be lower than orthogonal to the layers.

A similar behaviour can be observed at the results for D2. Figure 10 shows the stress-strain curve while Table 9 shows the average results (x) including standard deviation (s) of the D2 blend in X and Z direction compared to the targeted values from conventionally manufactured 1.4501. The Young´s Modulus is low for the X-specimen but the other values are within the tolerances and similar range like the other specimens.

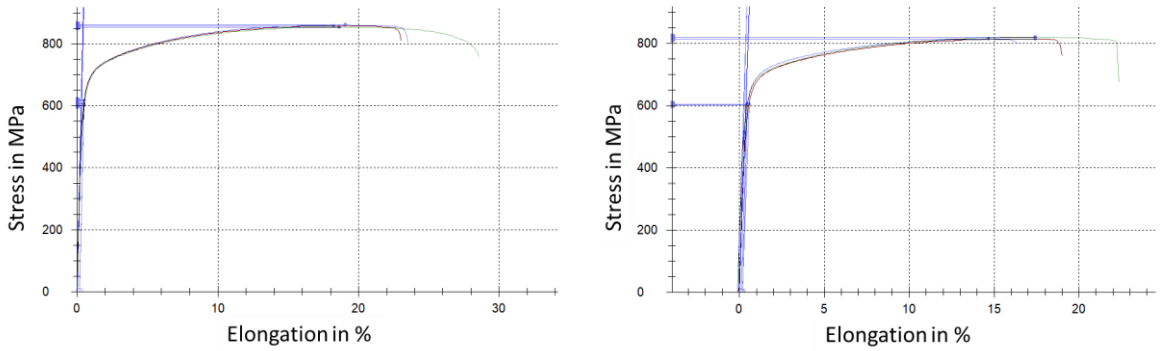

Figure 9. Stress-strain curve of D1 – X (left) and D1 – Z (right)

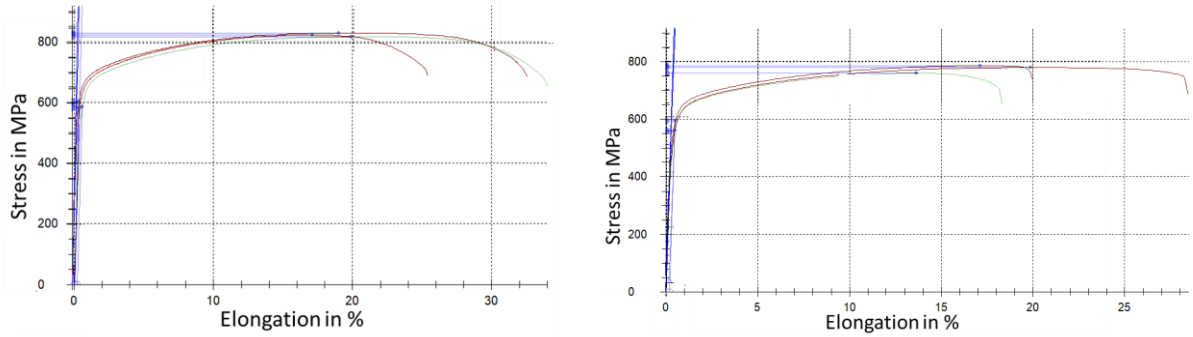

Figure 10. Stress-strain curve of D2 – X (left) and D2 – Z (right)

Table 8: Results of tensile tests of D1 in X and Z direction

D1 - X	YMod [kN/mm²]	Rp 0.2 [N/mm²]	Rm [N/mm²]	Agt [%]
n = 3				
x	199,40	608,16	858,26	18,66
s	13,72	8,32	3,30	0,43
Target (1.4501)	200	≥ 530	730 - 930	≥ 25

D1 - Z	YMod [kN/mm²]	Rp 0.2 [N/mm²]	Rm [N/mm²]	Agt [%]
n = 3				
x	181,93	602,59	815,83	16,55
s	25,97	1,60	3,55	1,60
Target (1.4501)	200	≥ 530	730 - 930	≥ 25

Table 9: Results of tensile tests of D2 in X and Z direction

D2 - X	YMod [kN/mm²]	Rp 0.2 [N/mm²]	Rm [N/mm²]	Agt [%]
n = 3				
x	168,82	583,11	819,86	18,54
s	13,27	3,40	3,46	1,88
Target (1.4501)	200	≥ 530	730 - 930	≥ 25

D2 - Z	YMod [kN/mm²]	Rp 0.2 [N/mm²]	Rm [N/mm²]	Agt [%]
n = 3				
x	198,03	559,87	770,65	16,77
s	2,83	1,81	13,99	4,41
Target (1.4501)	200	≥ 530	730 - 930	≥ 25

Conclusions

In this study two different metal powder blends were processed by LPBF and compared to specimen made of prealloyed powder and conventionally manufactured parts. The investigation focused on the

homogeneity of the parts and the dependent corrosion resistance and tensile strength.
Following conclusions can be drawn from the work:

- The parts built by using the powder blends were built successfully with LPBF and the chemical composition suits the analysed and calculated powder composition, respectively.
- Some non-melted particles can appear locally.
- Diffusion annealing can reduce inhomogeneity and improves corrosion resistance.
- The LPBF process itself has a big influence on corrosion behaviour, especially porosity.
- The tensile tests show that the parts can be loaded as much as the conventionally manufactured parts, since the tensile strength is within the tolerances of the material. Only the elongation is slightly lower.

Additional research needs to be carried out to identify a parameter set for stable chemical and microstructural homogeneity of each position on the samples. To bring these alloys into industrial application a reliable process with homogeneous parts is required. Further studies should include a systematic analysis of the heat treatment conditions and the resulting mechanical properties. The heat treatment can possibly lead to a more reliable microstructure.

Acknowledgements

The work presented was funded by IGF project 20933N of the “Forschungsgesellschaft Stahlverformung e.V.” via the AiF as part of the IGF program by the Bundesministerium für Wirtschaft und Energie.

References

1. The corrosion of superduplex stainless steel in different types of seawater. Francis, Ruthie & Byrne, Glenn & Warburton, Geoffrey. s.l. : NACE - International Corrosion Conference Series, 2011.
2. Mohammad Hossein Mosallanejad, Behzad Niroumand, Alberta Aversa, Abdollah Saboori. In-situ alloying in laser-based additive manufacturing processes: A critical review. Journal of Alloys and Compounds . 2021, Bd. Volume 872.
3. Clayton, R. M. The use of elemental powder mixes in laser-based additive manufacturing. Missouri : Missouri University of Science and Technology, 2013.
4. C. Haase, F. Tang, M. Wilms, A. Weisheit und B. Hallstedt. Combining thermodynamic modeling and 3D printing of elemental powder blends for high-throughput investigation of high-entropy alloys - Towards rapid alloy screening and design. Materials Science & Engineering. 2017, S. Bd. 688, pp. 180-189.
5. W. Li, X. Chen, L. Yan, J. Zhang, X. Zhang und F. Liou. Additive manufacturing of a new Fe-Cr-Ni alloy with gradually changing compositions with elemental powder mixes and thermodynamic calculation. Journal of Advanced Manufacturing Technologies. 2018, S. Bd. 95, pp. 1013-1023.
6. Influence of Powder Properties on the Mixing Behaviour of Metal Powders in LPBF. Michael Norda, Marie Luise Köhler. Digital Conference : s.n., 2021. EuroPM.
7. Shenoy, P. Dry mixing of spice powders investigation of effect of powder properties on mixture quality of binary powder mixtures. s.l. : University College Cork, 2014.
8. Thermocalc Website. [Online] [Zitat vom: 25. 04 2022.] https://thermocalc.com/.
9. Satir, Anne and Feichtinger, Heinrich. On the solubility of Nitrogen in liquid iron and steel alloys using elevated pressure. Zeitschrift fuer Metallkunde 52. 09 1991, S. 689.
10. THC Childs, C. Hauser, and M. Badrossamay. Selective laser sintering (melting) of stainless and tool steel powders: experiments and modelling. Proceedings of the Institution of Mechanical Engineers, Part B: Journal of Engineering Manufacture. 2005, S. 219(4):339-357.
11. Corrosion behavior of 316L austenitic steel processed by selective laser melting, hot-isostatic pressing, and casting. K. Geenen, A. Rottger, W. Theisen. 2017, Mater. Corros. 68, S. 764-775.
12. Amol B. Kale, Byung-Kyu Kim, Dong-Ik Kim, E.G. Castle, M. Reece, Shi-Hoon Choi. An investigation of the corrosion behavior of 316L stainless steel fabricated by SLM and SPS techniques. Materials Characterization. 2020, Bd. Volume 163.
13. Houbaert, T. Ros-Yañez and Y. High-silicon steel produced by hot dipping and diffusion annealing. Journal of Applied Physics 91. 13. May 2002.
14. Saeidi K, Alvi S, Lofaj F, Petkov VI, Akhtar F. Advanced Mechanical Strength in Post Heat Treated SLM 2507 at Room and High Temperature Promoted by Hard/Ductile Sigma Precipitates. Metals 2019;9:199.
15. Decheng Kong, Xiaoqing Ni, Chaofang Dong, Liang Zhang, Cheng Man, Xuequn Cheng, Xiaogang Li. Anisotropy in the microstructure and mechanical property for the bulk and porous

316L stainless steel fabricated via selective laser melting. Materials Letters Volume 235. January 2019, S. 1-5.